Journal of Materials Chemistry B

Accepted Manuscript

ROYAL SOCIETY OF CHEMISTRY

www.rsc.org/materialsB

Journal of Materials Chemistry B

ARTICLE

Polyphosphoester-conjugated camptothecin prodrug with disulfide linkage for potent reduction-triggered drug delivery

Received 00th January 20xx,
Accepted 00th January 20xx

DOI: 10.1039/x0xx00000x

www.rsc.org/

Qingqing Zhang, Jinlin He,* Mingzu Zhang and Peihong Ni*

A new kind of reduction-cleavable polymer-camptothecin (CPT) prodrug has been developed, in which the polymer backbone consisted of a biodegradable diblock polyphosphoester (PBYP-*b*-PEEP), and a modified CPT was linked onto the pendant alkynes of PBYP *via* Cu(I)-catalyzed azide-alkyne cycloaddition (CuAAC) "click" reaction to yield the polymeric prodrug, abbreviated as (PBYP-*g*-*ss*-CPT)-*b*-PEEP. The resulting prodrug could self-assemble into uniform prodrug micelles in aqueous solution. Since the releasable disulfide carbonate between CPT and polyphosphoester would be disrupted under an intracellular reducing environment, the disassociation of prodrug micelles could result in a rapid release of the CPT parent drug. The chemical structures of the intermediate polymers and polymeric prodrug have been fully characterized by ^{1}H NMR and FT-IR analyses, while the molecular weights and molecular weight distributions were measured by gel permeation chromatography (GPC). The self-assembly behavior of the prodrug was investigated by the fluorescence probe method, dynamic light scattering (DLS) and transmission electron microscopy (TEM) analyses. The DLS results indicated that these prodrug micelles were relatively stable in neutral pH media, but could be degraded under the reductive condition. The *in vitro* drug release studies showed that the CPT release from prodrug micelles was proceeded in a glutathione (GSH)-dependent manner. A methyl thiazolyl tetrazolium (MTT) assay demonstrated that the prodrug micelles could efficiently inhibit the proliferation of HepG2 cells. In addition, the intracellular uptake of prodrug micelles could efficiently release CPT into HepG2 cells, which was obsered by a live cell imaging system. All these results indicated that this GSH-responsive polymeric prodrug is highly potential in reduction-triggered cancer chemotherapy.

Introduction

Chemotherapy is one of the most commonly used therapeutic approaches for cancer treatment. However, it is usually restricted because most of the small molecule anticancer agents, such as the clinically widely applied doxorubicin (DOX), camptothecin (CPT), and paclitaxel (PTX), have poor water solubility, nonselectivity and serious adverse effects.[1,2] To this end, inspired by the integration of polymeric nanotechnology with modern medicine,[3] tremendous progresses have been made in the field of macromolecular drug delivery systems, including micelles,[4,5] polymersomes,[6] nanogels,[7] and polymeric prodrugs.[8-10] Since Ringsdorf first proposed the concept of macromolecular drugs in 40 years ago,[11] which was also named as the polymer-drug conjugates or prudrugs, a variety of prodrug systems have been developed by covalently conjugating chemotherapeutic agents to polymers,[12-16] and some of them are now advanced to different stages of clinical trials.[10,17] This strategy can not only overcome some limitations associated with small molecule chemotherapeutic drugs, but also greatly improve drug bioavailability *via* either passive targeting by the enhanced permeability and retention (EPR) effect[18,19] or active targeting by introducing some specific tumor-homing ligands.[20,21] As compared to the physical encapsulation of drugs into polymeric nanoparticles, polymeric prodrugs usually preserve the advantages of nanosized drug carriers, improve the drug loading content and loading efficiency, and can prevent undesirable premature drug release during storage and blood circulation.

In recent years, increasing efforts have been dedicated to the development of intracellular stimuli-responsive nanocarriers that are generally stable under extracellular conditions (e.g., in blood circulation) but rapidly release the loaded payloads after entering into tumor cells, resulting in markedly enhanced therapeutic efficacy.[5,22,23] The anticancer drugs can be covalently installed in polymer chains through cleavable linkages that are capable of degrading triggered by the environmental stimuli, such as pH,[24-26] redox,[27-29], light irradiation,[30,31] and enzyme.[32] In particular, researchers have paid much more attention to the disulfide bond as a linkage of the polymeric prodrugs because it can be cleaved in the presence of reducing agents.[33] Glutathione (GSH) is the most abundant biological reducing agent in body. It has been demonstrated that the body fluids (e.g., blood) and normal extracellular matrices possess a low GSH concentration (2-20 μM), while the cytosol and nucleus have a high redox potential

College of Chemistry, Chemical Engineering and Materials Science, Suzhou Key Laboratory of Macromolecular Design and Precision Synthesis, Jiangsu Key Laboratory of Advanced Functional Polymer Design and Application, Soochow University, Suzhou 215123, P. R. China. Tel: +86 512 65882047; E-mail: phni@suda.edu.cn (P. Ni) and jlhe@suda.edu.cn (J. He)

with GSH concentrations ranging from 2 to 10 mM.[22,23,34] Meanwhile, it should further be emphasized that the tumor tissues and cytosol are also found to possess at least 4-fold higher concentrations of GSH than those in normal tissues.[35,36] Therefore, the unique concentration gradient of GSH is useful to construct the reduction-responsive polymeric delivery systems for active drug release inside tumor cells as well as in tumor tissues.[37-39]

Camptothecin (CPT), originally isolated from Camptotheca acuminate, is a potent broad-spectrum anticancer agent that inhibits type I DNA topoisomerase to induce apoptosis in rapidly dividing tumor cells.[40,41] However, the application of CPT as a therapeutic agent has been severely hampered by its poor aqueous solubility, which can lead to rapid blood clearance and unpredictable efficacy (e.g., myelosuppression and gastrointestinal toxicity) following intravenous administration.[41] During the circulation in blood, which is weakly alkaline and contains abundant serum albumin, the therapeutically active lactone of CPT tends to open the lactone ring to generate the inactive and toxic carboxylate species.[41-43] In addition, serum albumin can preferentially bind to the carboxylate form which strongly forces lactone-carboxylate equilibrium toward the formation of the carboxylate.[44] To address these challenges, CPT has been successfully conjugated to a variety of polymers, such as poly (L-succinimide),[29] polyethylene glycol,[45-47] poly[*N*-(2-hydroxypropyl) methacrylamide],[48] dextran,[49] poly(L-glutamic acid),[50] poly(2-methacryloyloxyethyl phosphorylcholine),[51] and poly[tyrosine(alkynyl)-OCA].[52]

Herein, we report on a novel polymeric prodrug based on polyphosphoester-CPT conjugate, that is, (PBYP-*g*-*ss*-CPT)-*b*-PEEP, in which the connection of CPT molecule and polyphosphoester backbone was achieved by a releasable disulfide carbonate linkage. This kind of polymeric prodrug was designed on the basis of following considerations: (i) polyphosphoesters (PPEs) are appealing materials for potential biological applications because of their good biocompatibility and biodegradability, as well as their structural versatility.[53-55] Moreover, it has been proved that phosphodiesterase I (PDE I), a well-known enzyme present in the cytosome or subcellular regions of human cells, can accelerate the degradation of PPEs;[56] (ii) the highly efficient CuAAC "click" reaction was used to graft CPT derivative onto the PPE backbone to ensure the controlled loading content of drug; (iii) a disulfide carbonate linkage is introduced to endow the prodrug with the property of efficiently releasing CPT parent drug *via* the intracellular disulfide reduction.[27,52] As shown in Scheme 1, the resulting (PBYP-*g*-*ss*-CPT)-*b*-PEEP is an amphiphilic polymeric prodrug and can self-assemble into micelles in aqueous solution. When these micelles enter into cancer cells by passive tumor targeting, PDE I will accelerate the degradation of PPE backbone and the disulfide carbonate linkage would be rapidly cleaved under reducing microenvironment, thus leading to a fast release of CPT parent drug.

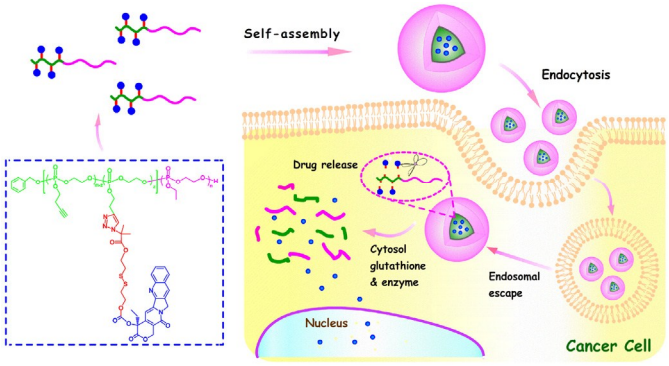

Scheme 1. Schematic illustration of the reduction-sensitive micelles self-assembled from amphiphilic polymeric prodrug (PBYP-*g*-*ss*-CPT)-*b*-PEEP for the efficient intracellular release of CPT triggered by the reductive microenvironment inside cancer cell.

Experimental

Materials

2, 2'-dithiobis[1-(2-bromo-2-methyl-propionyloxy)ethane] (HO-ss-Br) was synthesized according to a previously reported method.[57] 2-Ethoxy-2-oxo-1,3,2-dioxaphospholane (EOP)[16,39,58] and 2-(but-3-yn-1-yloxy)-2-oxo-1,3,2-dioxaphospholane (BYP)[59-62] were prepared by the previously reported protocols. Camptothecin (CPT, 99%, Beijing Zhongshuo Pharmaceutical Technology Development), triphosgene (99%, J&K Chemical), sodium azide (NaN_3, A.R., Sinopharm Chemical Reagent), 2, 2'-dithiodiethanol (technical grade, Sigma-Aldrich), α-bromoisobutyryl bromide (98%, Sigma-Aldrich), 4-dimethylaminopyridine (DMAP, 99%, Shanghai Medpep), acetonitrile (HPLC grade, Sinopharm Chemical Reagent), and 2, 2'-dipyridyl (bpy, 99%, Sinopharm Chemical Reagent) were used without further purification. Stannous octoate [$Sn(Oct)_2$, 95%, Sigma-Aldrich] was purified by distillation under reduced pressure prior to use. Dichloromethane (CH_2Cl_2, A.R.), triethylamine (TEA, A.R.) and benzyl alcohol (BzOH, A.R.) were purchased from Sinopharm Chemical Reagent and distilled before use. *N*, *N*-Dimethyl-formamide (DMF, A.R., Sinopharm Chemical Reagent) was dried over $MgSO_4$ and distilled under reduced pressure before use. Tetrahydrofuran (THF, A.R., Sinopharm Chemical Reagent) was initially dried over potassium hydroxide for at least two days and then refluxed over sodium wire with benzophenon as an indicator until the color turned purple. Cuprous bromide (CuBr, 95%, Sinopharm Chemical Reagent) was successively washed three times with glacial acetic acid and acetone, followed by drying for 12 h under vacuum at room temperature. Milli-Q water (18.2 MΩ cm^{-1}) was generated using a water purification system (Simplicity UV, Millipore). All the cell culture related reagents were purchased from Invitrogen.

Synthesis of 2, 2'-dithiobis[1-(2-azido-2-methyl-propionyloxy) ethane] (HO-*ss*-N_3)

Following a procedure reported in the literature,[57] HO-*ss*-Br was first synthesized by the monoesterfication of 2, 2'-dithiodiethanol with α-bromoisobutyryl bromide. Subsequently, HO-*ss*-Br (1.36 g, 4.5 mmol) and NaN_3 (0.58 g, 9.0 mmol) were added into one 50 mL of flask containing 10 mL of DMF. The reaction was performed at 30 °C for 40 h. The mixture was passed through a short column of basic Al_2O_3 to remove the residual NaN_3 and the solution was evaporated to remove DMF. The crude product was dissolved in 100 mL of distilled water and extracted with CH_2Cl_2 for three times. The organic layer was dried over anhydrous Na_2SO_4 for 4 h and the filtrate was dried by rotary evaporation. Finally, the product was dried under vacuum at 25 °C for 24 h to give a transparent viscous liquid (HO-*ss*-N_3, 1.13 g, yield: 95 %). ^{1}H NMR (DMSO-d_6, 400 MHz, ppm): δ 1.44 (s, 6H, –COC(C***H***$_3$)N_3), δ 2.81 (t, 2H, HOCH$_2$C***H***$_2$S–), δ 3.02 (t, 2H, –SC***H***$_2$CH$_2$–), δ 3.63 (q, 2H, HOC***H***$_2$CH$_2$–), δ 4.39 (t, 2H, –CH$_2$C***H***$_2$O–), δ 4.88 (t, 1H, –O***H***).

Synthesis of reduction-responsive and clickable CPT derivative CPT-*ss*-N_3

CPT (1.0 g, 2.87 mmol) and DMAP (1.05 g, 8.65 mmol) were suspended in 150 mL of dry CH_2Cl_2 under a dry argon atmosphere. Triphosgene (0.28 g, 0.96 mmol) was then added at 5 °C and the mixture was stirred at this temperature for 30 min. After that, a solution of HO-*ss*-N_3 (1.13 g, 4.26 mmol) in 15 mL of dry THF was added dropwise into the reactor through a constant-pressure funnel. The reaction mixture was further stirred at 5 °C for 12 h. After filtration and removing all the solvents by rotary evaporation, the residue was diluted with 100 mL of CH_2Cl_2 and washed with water, 1.0 M HCl solution, and brine, respectively. The organic layer was collected and dried over anhydrous Na_2SO_4 for 2 h. The filtrate was concentrated and the crude product was purified by silica column chromatography using ethyl acetate as the eluent to give a pale yellow powder (CPT-*ss*-N_3, TLC R_f = 0.57, 0.87 g, yield: 47%).

Synthesis of diblock copolymer PBYP-*b*-PEEP

The poly(butynyl phospholane)-*block*-poly(ethylethylene phosphate) (PBYP-*b*-PEEP) diblock copolymer was synthesized *via* the "one-pot" sequential ring-opening polymerization (ROP) of BYP and EOP monomers, using BzOH as the initiator and Sn(Oct)$_2$ as the catalyst. A typical preparation route is described as follows: a 50 mL of round-bottomed flask equipped with a magnetic stirring bar was charged with BzOH (0.035 g, 0.35 mmol), BYP (1.25 g, 7.1 mmol), and 5 mL of anhydrous CH_2Cl_2 under a dry nitrogen atmosphere. A solution of Sn(Oct)$_2$ (0.14 g, 0.35 mmol) in 0.2 mL of anhydrous toluene was quickly injected into the flask by syringe. After stirring at 30 °C for 1 h, 0.5 mL of the reaction mixture was withdrawn to determine the conversion of BYP by ^{31}P NMR measurement. Subsequently, EOP (4.43 g, 30 mmol) was injected into the flask by syringe and the reaction was carried out at 30 °C for 3 h. Afterwards, the mixture was concentrated under reduced pressure and precipitated in a mixed solvent of cold diethyl ether/methanol (10/1, v/v) twice. The precipitate was then collected and dried under vacuum at 25 °C for 24 h (PBYP-*b*-PEEP, 4.50 g, yield: 79%). ^{1}H NMR ($CDCl_3$, 400 MHz, ppm): δ 1.31-1.44 (t, 246H, –CH$_2$C***H***$_3$), δ 2.04-2.17 (s, 16H, ≡C***H***), δ 2.56-2.67 (t, 32H, –C***H***$_2$C≡CH), δ 3.79 (t, 2H, –C***H***$_2$OH), δ 4.10-4.21 (m, 196H, –C***H***$_2$CH$_2$C≡CH, –C***H***$_2$CH$_3$), δ 4.21-4.37 (t, 390H, –OC***H***$_2$C***H***$_2$O–, –OC***H***$_2$CH$_2$OH), δ 5.10 (s, 2H, C$_6$H$_5$C***H***$_2$–), δ 7.4 (d, 5H, C$_6$***H***$_5$–).

Synthesis of polymeric prodrug (PBYP-*g*-*ss*-CPT)-*b*-PEEP

The polymeric prodrug (PBYP-*g*-*ss*-CPT)-*b*-PEEP was synthesized *via* the CuAAC "click" reaction between PBYP-*b*-PEEP and CPT-*ss*-N_3. Briefly, PBYP-*b*-PEEP (0.5 g, 0.52 mmol of alkynyl group) and CPT-*ss*-N_3 (167 mg, 0.26 mmol of azide group) were dissolved in 10 mL of anhydrous CH_2Cl_2 in a 50 mL of nitrogen-purged flask. Subsequently, CuBr (38 mg, 0.26 mmol) and bpy (82 mg, 0.52 mmol) were sequentially added into the flask, and the mixture was degassed through three exhausting-refilling nitrogen cycles. The mixture was stirred at 35 °C for 24 h under a nitrogen atmosphere. After exposing to air to terminate the reaction, the reaction mixture was diluted with 250 mL of CH_2Cl_2, passed through a short column of basic Al_2O_3. The solution was concentrated under reduced pressure and precipitated into cold diethyl ether twice. The precipitate was then collected and dried under vacuum at 25 °C for 24 h [(PBYP-*g*-*ss*-CPT)-*b*-PEEP, 0.40 g, yield: 60%]. The residual copper content was measured to be about 0.49 ppm by atomic absorption spectrometry (AAS), indicating that most of the copper residue was efficiently removed after purification.

Characterizations

^{1}H NMR and ^{31}P NMR spectra were recorded on a 400 MHz nuclear magnetic resonance (NMR) instrument (INOVA-400, Varian) using $CDCl_3$ or DMSO-d_6 as the solvent. The number-average molecular weights and molecular weight distributions (PDIs) of polymers were analyzed by a gel permeation chromatography (GPC) instrument (HLC-8320, Tosoh) equipped with two TSKgel Super HM-M columns (6.0 × 150 mm, 3 μm particle size) in series with molecular weights ranging from 1 × 10^3 to 7 × 10^5 g mol^{-1} and a refractive index detector. DMF containing 0.05 mol L^{-1} of LiBr was used as the eluent at a flow rate of 0.60 mL min^{-1} at 40 °C. A series of narrowly distributed polystyrene standards were used as the calibration. Fourier transform infrared (FT-IR) spectra were recorded on a Nicolet 6700 spectrometer using the KBr disk method. The UV-Vis absorption spectra were measured on a UV-Vis spectrophotometer (UV-2550, Shimadzu). The mass spectra were performed on a 1260-6120 LC/MS instrument (Agilent) with acetonitrile as the solvent.

HPLC analysis

The CPT derivatives and prodrug were determined by a reverse phase high performance liquid chromatography (HPLC) (UltiMate 3000, Thermo Fisher Scientific) equipped with a UltiMate pump, a controller, an autosampler, and a UV detector conducted at 254 nm. The samples were analyzed on a C_{18} reverse phase column (4.6 × 100 mm, 5 μm particle size) at 30 °C with acetonitrile-Milli-Q water (75/25, v/v) as the

mobile phase at a flow rate of 1.0 mL min^{-1}. The data was analyzed by Chromleon 7 software.

Self-assembly behavior

To estimate the critical aggregation concentration (CAC) values of polymeric prodrug (PBYP-*g*-*ss*-CPT)-*b*-PEEP, Nile red was used as the fluorescence probe. Typically, a predetermined Nile red solution in CH_2Cl_2 was added into a series of ampoules. After CH_2Cl_2 was evaporated under reduced pressure, 5 mL of the prodrug solutions in Milli-Q water with different concentrations were respectively added into each ampoule. The final concentration of Nile red in each ampoule was 1×10^{-6} mol L^{-1}. The samples were sonicated for 15 min and vigorously stirred at room temperature for 48 h. The mixtures were recorded on a spectrofluorometer (FLS920, Edinburgh) at the excitation wavelength of 485 nm and emission spectra were recorded ranging from 550 to 700 nm. Both the slit width for excitation and emission were set at 2 nm. The fluorescence intensity from the emission spectra was analyzed as a function of the logarithm concentrations of polymeric prodrug. The CAC value was determined as the crossover point of the two lines in the plot of fluorescence versus polymer concentration.

The micelles self-assembled from (PBYP-*g*-*ss*-CPT)-*b*-PEEP were prepared by directly dissolving the sample into Milli-Q water at a concentration of 0.5 mg mL^{-1}. The solution was sonicated for at least 30 min and vigorously stirred for 48 h. The average particle sizes ($\bar{D}_z$) and size polydispersity indices (size PDIs) of the prodrug micelles were determined by a dynamic light scattering (DLS) instrument (Zetasizer Nano ZS, Malvern). The morphologies of micelles were observed by a transmission electron microscope (TEM) instrument (HT7700, Hitachi) operated at an accelerating voltage of 120 kV. Samples for TEM were prepared by a freeze-drying method.[63] The carbon-coated copper grid was placed on the bottom of a glass dish, which was then immediately inserted into liquid nitrogen. Subsequently, 10 μL of the micellar solution was dripped onto the grid, and the solvent in its frozen solid state was directly removed without melting in a freeze-drier. The morphologies were then imaged on the TEM instrument at room temperature.

***In vitro* CPT release from P(BYP-*g*-*ss*-CPT)-*b*-PEEP**

The release of CPT parent drug from (PBYP-*g*-*ss*-CPT)-*b*-PEEP micelles with an equivalent CPT concentration at 50 μg mL^{-1} were investigated at 37 °C in four kinds of buffer solutions: (a) phosphate buffer solution (10 mM, pH 7.4), (b) phosphate buffer solution (10 mM, pH 7.4) with 2 μM GSH, (c) phosphate buffer solution (10 mM, pH 7.4) with 5 mM GSH, and (d) phosphate buffer solution (10 mM, pH 7.4) with 10 mM GSH.

In brief, 25 mg of (PBYP-*g*-*ss*-CPT)-*b*-PEEP was dissolved in 50 mL of PBS and stirred for 12 h, 5 mL of the solution was then transferred into a dialysis membrane (MWCO 12 kDa), which was immersed into 20 mL of the corresponding buffer solutions and incubated at 37 °C with constant shaking. At predetermined intervals, 5 mL of the dialysis medium was withdrawn and replenished with an equal volume of the corresponding fresh buffer solution. The CPT concentration was determined by spectrofluorometer with excitation at 375 nm and emission at 430 nm, and the slit width was set at 2 nm. All the release experiments were conducted in triplicate and the reported results were the average values with standard deviations.

***In vitro* cytotoxicity**

HepG2 and L929 cells were obtained from American Type Culture Collection (ATCC), and incubated in DMEM supplemented with 10% FBS and 1% of penicillin/streptomycin. The culture media were replaced every 3 days. The cells were cultured at 37 °C under a humidified atmosphere containing 5% CO_2 and used in their growth state. A standard methyl thiazolyl tetrazolium (MTT) assay was used to evaluate the cytotoxicity of the PBYP-*b*-PEEP and (PBYP-*g*-*ss*-CPT)-*b*-PEEP against both HepG2 and L929 cells, using free CPT as the control. Cells were seeded into 96-well plates at a density of 1×10^4 cells per well. Cells were allowed to attach overnight in a humidified atmosphere of 5% CO_2 at 37 °C before exposed to the samples at different concentrations. After 48 h of incubation, 25 μL of MTT stock solution (5 mg mL^{-1} in PBS) was added to each well. Subsequently, cells were incubated at 37 °C for additional 4 h allowing the viable cells to reduce the MTT into purple formazan crystals. DMEM medium was removed and 150 μL of DMSO was added to each well. Finally, the absorbance at 570 nm of each well was measured using a microplate reader (Bio-Rad 680) to obtain the optical density (OD) value. The relative cell viability was calculated according to the formula: cell viability (%) = $(OD_{treated}/OD_{control}) \times 100$, where $OD_{treated}$ represents the OD value obtained in the presence of samples, and $OD_{control}$ is the value that acquired in the absence of samples.

Cellular uptake and intracellular release of CPT

The cellular uptake of free CPT and CPT prodrug against HepG2 cells were investigated by a live cell imaging system (Cell'R, Olympus) and the intracellular observation of CPT was detected at an excitation wavelength of 385 nm. HepG2 cells routinely maintained in DMEM supplemented with 10% FBS and 1% of penicillin/streptomycin were seeded in a 96-well plate at a density of 2×10^4 cells per well. The culture dish was mounted in the incubation system of the live cell imaging system at 37 °C under 5% CO_2 atmosphere. Afterwards, the culture medium was removed and cells were carefully washed with PBS, followed by staining with NucRed™ Live 647 (1 drop mL^{-1}) for 15 min and washing with PBS again. Finally, 1 mL of fresh culture medium containing free CPT or CPT prodrug (the final concentration of CPT was 0.5 mg L^{-1}) was added. The images were then captured with the excitation wavelength of 560 nm (red) and 385 nm (blue).

Results and discussion

Structural characterizations

As shown in Scheme 2, the reduction-responsive polymeric prodrug (PBYP-*g*-*ss*-CPT)-*b*-PEEP was synthesized *via* the following steps: (A) synthesis of an azide-functionalized reduction-responsive CPT derivative (CPT-*ss*-N_3); (B) preparation of a polyphosphoester-based diblock copolymer PBYP-*b*-PEEP, and final formation of the polymeric prodrug (PBYP-*g*-*ss*-CPT)-*b*-PEEP by the CuAAC "click" reaction between CPT-*ss*-N_3 and PBYP-*b*-PEEP. The proposed mechanism for the reduction-trigered release of CPT parent drug is shown in Scheme 2(C). The disulfide carbonate group in (PBYP-*g*-*ss*-CPT)-*b*-PEEP can be cleaved under the reductive milieu and generate a thiol-containing intermediate. Subsequently, the carbonate bond in this intermediate can be quickly attacked by the thiol group, thus releasing a five-membered thiolactone and the CPT parent drug.

The chemical structure of CPT-*ss*-N_3 was verified by ^{1}H NMR, ^{13}C NMR, FT-IR, HPLC, and LC/MS analysis. Fig. 1 shows the ^{1}H NMR spectra of HO-*ss*-Br, HO-*ss*-N_3, and CPT-*ss*-N_3, respectively, while the ^{13}C NMR spectrum of CPT-*ss*-N_3 is shown Fig. 2. All the characteristic peaks ascribed to the protons and carbon atoms in the corresponding chemical structure can be found in the spectra. The clickable HO-*ss*-N_3 was synthesized by a nucleophilic substitution reaction of the HO-*ss*-Br with NaN_3. Compared with the ^{1}H NMR spectrum of HO-*ss*-Br in Fig. 1(A), it is noted that the peak at δ 1.90 ppm attributed to the methyl protons of [−(C***H***$_3$)$_2$CBr] disappeared completely, while a new peak at δ 1.43 ppm assigned to the methyl protons of [−(C***H***$_3$)$_2$CN$_3$] connected with an azide group appeared in Fig. 1(B), which confirmed the successful synthesis of clickable HO-*ss*-N_3. With the comparison of ^{1}H NMR spectrum of HO-*ss*-N_3 in Fig. 1(B), the spectrum of CPT-*ss*-N_3 in Fig. 1(C) exhibits new peaks attributed to the protons from CPT, while the proton signal of hydroxyl group (−CH$_2$O***H***) completely disappeared after reaction. In addition, FT-IR measurements were also used to characterize the samples and the results are shown in Fig. 3. The appearance of the absorption peak at 2108 cm^{-1} in Fig. 1(B) and Fig. 3(C) also indicated that the azide group was successfully introduced in CPT. Moreover, the results from HPLC analysis (the elution time for CPT is 3.33 min, and the value for CPT-*ss*-N_3 is 6.57 min). LC/MS further confirmed the chemical structure of CPT-*ss*-N_3 (calculated value for [M]$^+$: 639.15, found value for [M+H]$^+$: 640.15).

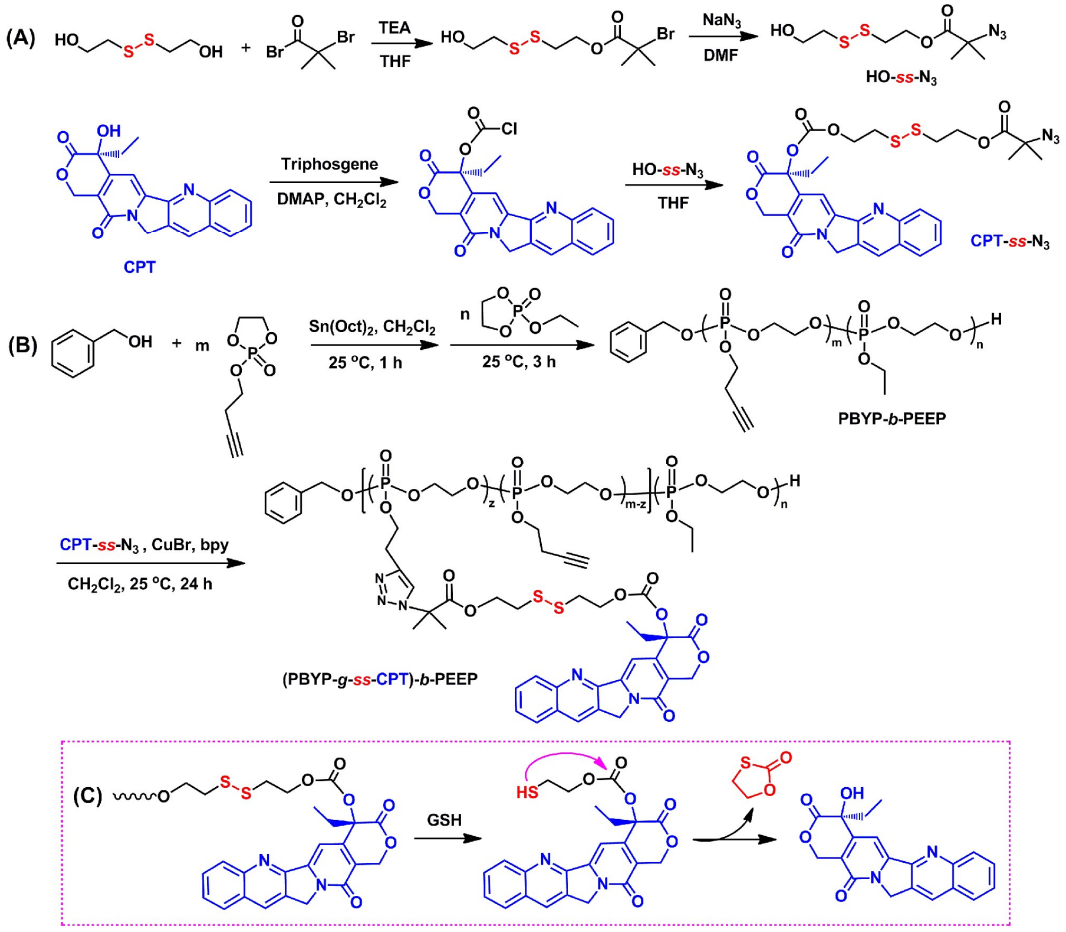

Scheme 2. Synthetic routes of (A) clickable CPT derivative CPT-*ss*-N_3 and (B) reduction-responsive polymeric prodrug (PBYP-*g*-*ss*-CPT)-*b*-PEEP; (C) mechanism of CPT release from (PBYP-*g*-*ss*-CPT)-*b*-PEEP in the presence of GSH.

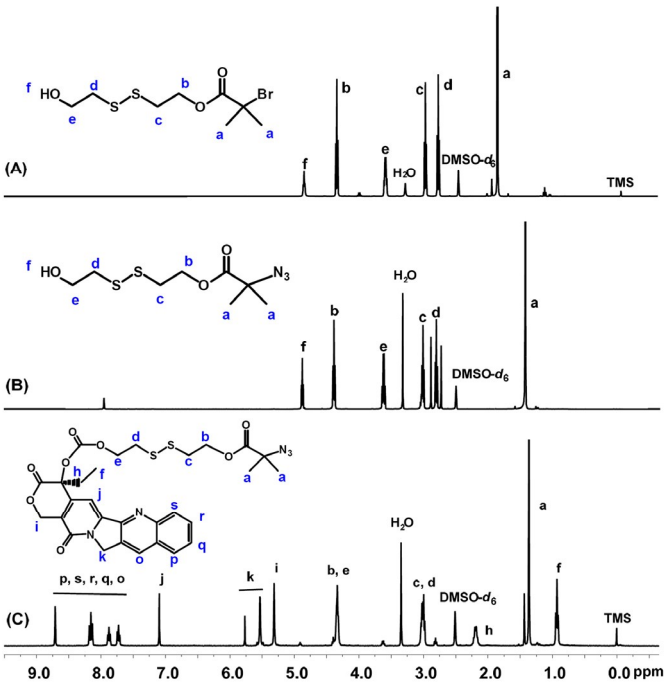

Fig. 1 ^{1}H NMR spectra of (A) HO-*ss*-Br, (B) HO-*ss*-N_3 and (C) CPT-*ss*-N_3 in DMSO-d_6.

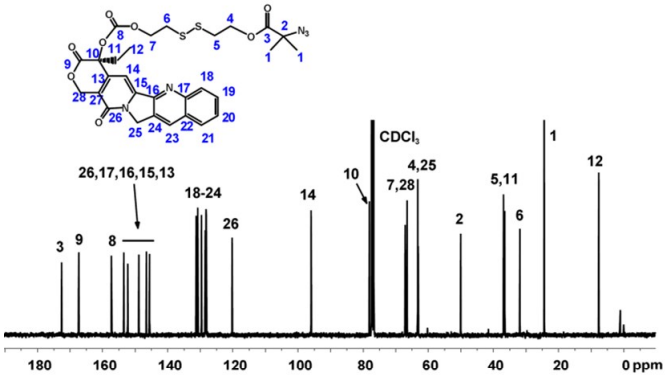

Fig. 2 ^{13}C NMR spectrum of CPT-*ss*-N_3 in $CDCl_3$.

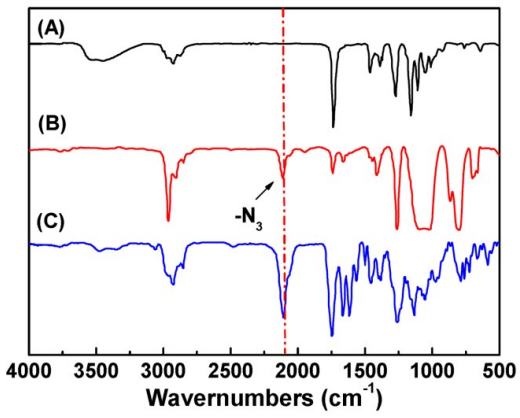

Fig. 3 FT-IR spectra of (A) HO-*ss*-Br, (B) HO-*ss*-N_3 and (C) CPT-*ss*-N_3.

The PBYP-*b*-PEEP block copolymers were synthesized in a sequential manner using BzOH as the initiator and $Sn(Oct)_2$ as the catalyst. After complete conversion of the first monomer BYP, the second monomer EOP was added into the reaction mixture. Fig. 4(A) displays the ^{31}P NMR spectrum of $PBYP_{16}$ reaction mixture without purification, and it is found that nearly 100% conversion of BYP was reached in 1 h of reaction. In addition, one can find that the spectrum of $PBYP_{16}$ has a strong peak at δ -1.68 ppm. For the ^{31}P NMR spectrum of $PBYP_{16}$-*b*-$PEEP_{82}$ copolymer as shown in Fig. 4(B), another strong peak appeared at δ -1.33 ppm, which can be assigned to the phosphorus atoms in the $PEEP_{82}$ backbone.

As shown in Scheme 2 (B), CPT-*ss*-N_3 was conjugated to the polyphosphoester units *via* the CuAAC "click" reaction. Fig. 5 shows the ^{1}H NMR spectra of $PBYP_{16}$-*b*-$PEEP_{82}$ and ($PBYP_{8.5}$-*g*-*ss*-$CPT_{7.5}$)-*b*-$PEEP_{82}$, from which all the signals assigned to the protons of the polymers can be observed. Compared with the ^{1}H NMR spectrum of $PBYP_{16}$-*b*-$PEEP_{82}$ in Fig. 5(A), the appearance of new signals attributed to the protons of CPT-*ss*-N_3 in Fig. 5(B) and peak 6' at δ 7.74 ppm attributed to the proton of the triazole ring was clearly detected. In addition, the peak attributed to the proton of methyl (-(CH_3)$_2$C-) of CPT-*ss*-N_3 at δ 1.50 ppm had shifted to δ 1.82 ppm after the click reaction. These results confirmed the successful synthesis of ($PBYP_{8.5}$-*g*-*ss*-$CPT_{7.5}$)-*b*-$PEEP_{82}$.

Based on the ^{1}H NMR spectrum in Fig. 5(A), the respective polymerization degrees (m and n) of PBYP and PEEP were respectively calculated by eqn (1) and (2), where A_2 is the integral area of the protons of the methylene group (peak 2, δ 5.06 ppm) in the benzyl segment, A_5 is the integral area of the protons of the methylene group adjacent to alkynyl (peak 5, δ 2.62 ppm) in the PBYP chain, and A_7 represents the integral area of methyl protons (peak 7, δ 1.36 ppm) in the PEEP chain. Based on the ^{1}H NMR spectrum in Fig. 5(B), the degree (z) of CPT derivative was calculated by eqn (3), where A_f is the integral area of the protons of methyl group (peak f, δ 1.01 ppm) in CPT.

$$m = \frac{A_5}{A_2} \quad (1)$$

$$n = \frac{2A_7}{3A_2} \quad (2)$$

$$z = \frac{A_7}{3A_f} \quad (3)$$

Therefore, the molecular weights of $PBYP_m$, $PBYP_m$-*b*-$PEEP_n$ and ($PBYP_{m-z}$-*g*-*ss*-CPT_z)-*b*-$PEEP_n$ could be obtained according to eqn (4) ~ (6), where 176.02, 152.02, 108.06 and 639.15 are the molecular weights of one repeating unit of PBYP, one repeating unit of PEEP, benzyl alcohol and CPT-*ss*-N_3, respectively. The letters (m, n and z) represent the numbers of the repeating units corresponding to the chemical structures.

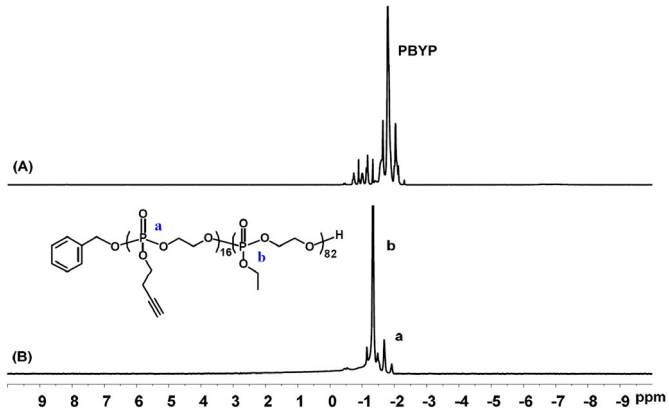

Fig. 4 ^{31}P NMR spectra of (A) $PBYP_{16}$ reaction mixture without purification and (B) purified $PBYP_{16}$-*b*-$PEEP_{82}$ in $CDCl_3$.

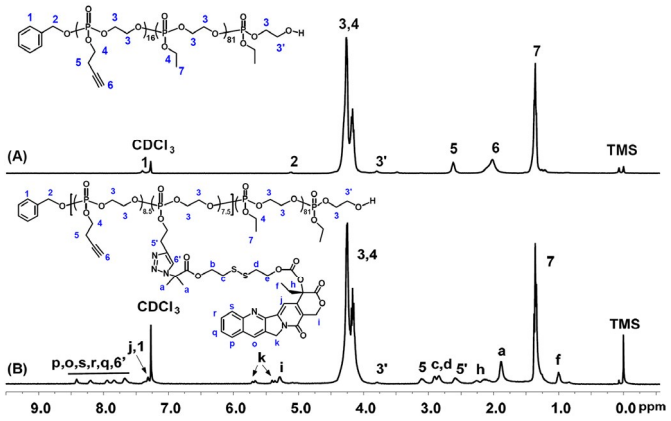

Fig. 5 ^{1}H NMR spectra of (A) $PBYP_{16}$-*b*-$PEEP_{82}$ and (B) ($PBYP_{8.5}$-*g*-*ss*-$CPT_{7.5}$)-*b*-$PEEP_{82}$ in $CDCl_3$.

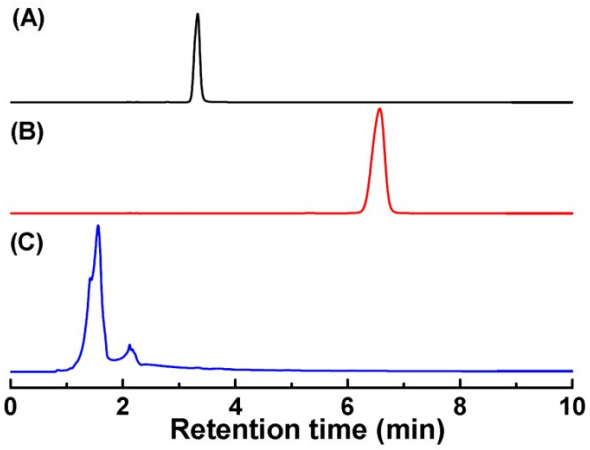

Fig. 6 HPLC analyses results of (A) free CPT, (B) CPT-*ss*-N_3 and (C) ($PBYP_5$-*g*-*ss*-CPT_3)-*b*-$PEEP_{26}$. HPLC analyses were performed with acetonitrile-water (75/25, v/v) as the mobile phase at 30 °C at a flow rate of 1.0 mL min^{-1}.

$$\overline{M}_{n,\,NMR\,(PBYP)} = m \times 176.02 + 108.06 \quad (4)$$

$$\overline{M}_{n,\,NMR\,(PBYP\text{-}b\text{-}PEEP)} = \overline{M}_{n,\,NMR\,(PBYP)} + n \times 152.02 \quad (5)$$

$$\overline{M}_{n,\,NMR\,(PBYP\text{-}g\text{-}ss\text{-}CPT)\text{-}b\text{-}PEEP} = \overline{M}_{n,\,NMR\,(PBYP\text{-}b\text{-}PEEP)} + z \times 639.15 \quad (6)$$

In addition, HPLC was also employed to distinguish (PBYP-*g*-*ss*-CPT)-*b*-PEEP and the HPLC traces are shown in Fig. 6, where the free CPT elutes at 3.33 min, CPT-*ss*-N_3 elutes at 6.57 min and the polymeric prodrug elutes at 1.56 min. Therefore, the results indicated that CPT-*ss*-N_3 was chemically conjugated to PBYP-*b*-PEEP.

The number-average molecular weights and molecular weight distributions (PDIs) of various polymers were measured by GPC analysis and the data are listed in Table 1. It should be noted that for the polyphosphoesters with relatively high molecular weight, the molecular weights determined by ^{1}H NMR and GPC analysis seem to have a big difference, which may be ascribed to the following reasons:[64,65] (1) the strong intermolecular interaction of polyphosphoesters chains occurred in DMF during GPC analysis; (2) there inevitably existed some deviations in the GPC measurement using polystyrene as the standard. Therefore, we could calculate the molecular weights according to the integral values from ^{1}H NMR spectra while obtain the PDI values from GPC analysis. In addition, GPC traces of representative homopolymer, diblock copolymer and polymeric CPT prodrug are illustrated in Fig. 7, in which all of them exhibit unimodal distribution, and no significant shoulder peaks are observed. Moreover, both of the traces of diblock copolymer and polymeric prodrug shift towards higher molecular weight side compared with that of homopolymer, indicating the growth of molecular weights and successful preparation. In addition, the CPT contents were determined by UV/Vis spectroscopy and the results are shown in Table 2. These results underlined the successful synthesis of (PBYP-*g*-*ss*-CPT)-*b*-PEEP.

Table 1. Molecular weight and molecular weight distribution of PBYP, PBYP-*b*-PEEP, and (PBYP-*g*-*ss*-CPT)-*b*-PEEP.

Samples	$\overline{M}_n$ [a] (g mol^{-1})	$\overline{M}_w$ [b] (g mol^{-1})	PDI [b]
$PBYP_8$-*b*-$PEEP_{26}$	5470	6750	1.17
($PBYP_5$-*g*-*ss*-CPT_3)-*b*-$PEEP_{26}$	7390	8740	1.23
$PBYP_{16}$	2920	2980	1.29
$PBYP_{16}$-*b*-$PEEP_{82}$	15280	29290	1.31
($PBYP_{10.2}$-*g*-*ss*-$CPT_{5.8}$)-*b*-$PEEP_{82}$	18990	35160	1.39
($PBYP_{8.5}$-*g*-*ss*-$CPT_{7.5}$)-*b*-$PEEP_{82}$	20070	38850	1.50

[a] Calculated by eqn (1)–(6) based on ^{1}H NMR analysis in $CDCl_3$. [b] Determined by GPC with DMF as the eluent and polystyrene as the standards.

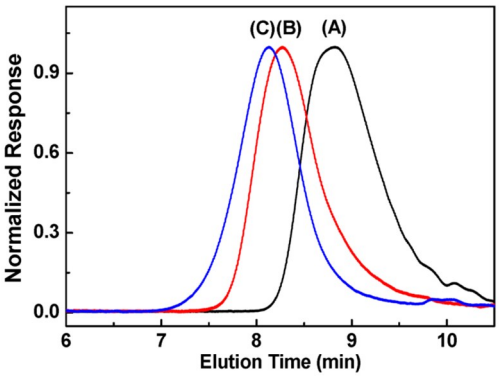

Fig. 7 GPC traces of (A) $PBYP_{16}$, (B) $PBYP_{16}$-*b*-$PEEP_{82}$ and (C) ($PBYP_{8.5}$-*g*-*ss*-$CPT_{7.5}$)-*b*-$PEEP_{82}$.

Table 2. The particle size and particle size distribution of micelles self-assembled from (PBYP-*g*-*ss*-CPT)-*b*-PEEP and their drug contents.

samples	CPT contents (wt%) [a]	Size (nm)	Size PDI
($PBYP_8$-*g*-*ss*-CPT_3)-*b*-$PEEP_{26}$	12.16	150	0.212
($PBYP_{10.2}$-*g*-*ss*-$CPT_{5.8}$)-*b*-$PEEP_{82}$	6.14	152	0.199
($PBYP_{8.5}$-*g*-*ss*-$CPT_{7.5}$)-*b*-$PEEP_{82}$	9.53	140	0.162

[a] Calculated by C_{CPT} (%) = $C_{UV\text{-}VIS}/C_{(PBYP\text{-}g\text{-}ss\text{-}CPT)\text{-}b\text{-}PEEP} \times 100$, where $C_{UV\text{-}VIS}$ represents the concentration of CPT measured by UV-VIS, while $C_{(PBYP\text{-}g\text{-}ss\text{-}CPT)\text{-}b\text{-}PEEP}$ is the concentration of prodrug sample.

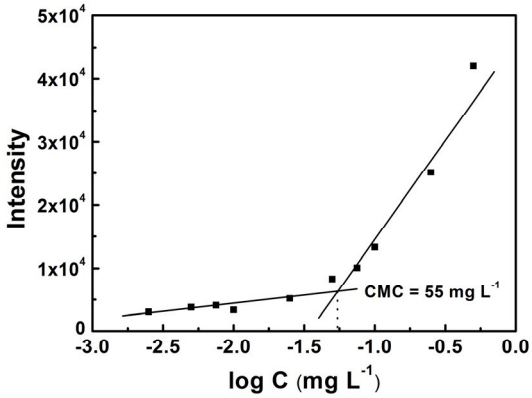

Fig. 8 Intensity of the fluorescence emission spectrum of Nile red as a function of logarithm concentration of ($PBYP_{8.5}$-*g*-*ss*-$CPT_{7.5}$)-*b*-$PEEP_{82}$ prodrug in aqueous solution.

Self-assembly of polymeric prodrug

The CPT prodrug (PBYP-*g*-*ss*-CPT)-*b*-PEEP can self-assemble into aggregates with hydrophobic PBYP segments conjugated CPT as the core and hydrophilic PEEP parts as the shell in aqueous solution once a critical concentration is exceeded. The micellization behavior of ($PBYP_{8.5}$-*g*-*ss*-$CPT_{7.5}$)-*b*-$PEEP_{82}$ in aqueous solution was determined by fluorescence spectroscopy using Nile red as a probe. From the result shown in Fig. 8, a critical micelle concentration (CMC) of 55 mg L^{-1} was estimated. The particle size and particle size distribution are important parameters of the nanocarriers for drug delivery. It is widely reported that drug-loaded nanoparticles with appropriate sizes less than 200 nm can extravasate into the tumor tissues *via* the leaky vessels by the EPR effect, and then release drugs into the vicinity of tumor cells.[66] DLS and TEM analyses were used to assess the self-assembly properties of the CPT prodrug. Generally, when the hydrophilic segment is longer than the hydrophobic block, the shape of the resulting micelles is spherical.[67] Fig. 9(A) shows the typical TEM image of micelles self-assembled by ($PBYP_{8.5}$-*g*-*ss*-$CPT_{7.5}$)-*b*-$PEEP_{82}$ (0.2 mg mL^{-1} in water), from which one can find that the micelles are spherical and the average size is less than 150 nm. The corresponding particle size distribution curve measured by DLS shown in Fig. 9(B) displays a monomodal peak with an average diameter of 140 nm and size PDI of 0.162. The particle sizes and size PDIs of the micelles formed by other polymeric prodrugs are summarized in Table 2. The differences between the average diameters of these micelles determined by DLS and TEM might be attributed to the hydrophilic PEEP segment, which can extend into the water phase during DLS measurement, while the hydrophilic chains tended to collapse in TEM analysis.

The disulfide carbonate linker was introduced to endow the (PBYP-*g*-*ss*-CPT)-*b*-PEEP micelles with a reduction-sensitive release mechanism of CPT. To demonstrate the functionality of this reduction-induced release mechanism, DLS was carried out to monitor the size change of prodrug micelles with 10 mM of GSH at different time intervals. It can be seen from Fig. 10 that a control experiment without GSH revealed unconspicuous change in the average particle size of the micelles over 24 h, indicating the favorable stability of prodrug micelles. In contrast, an obvious size change for ($PBYP_{8.5}$-*g*-*ss*-$CPT_{7.5}$)-*b*-$PEEP_{82}$ micelles was observed in the presence of 10 mM GSH, suggesting that variety of particle sizes were generated during the process of degradation. Within 4 h, the average particle size increased from 140 nm to about 410 nm with concomitant increase of the size PDI from 0.162 to 0.399. The large aggregates with an average diameter of >1000 nm were formed after 12 h. It can be concluded that the size increase was attributed to the cleavage of the disulfide linker in the presence of GSH. When CPT was cleaved from the backbone, the structure of the micelles became looser, and the looser micelles would further form large aggregates due to the inferior stability.

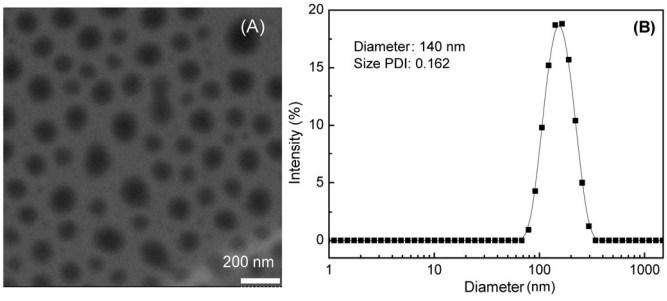

Fig. 9 (A) TEM image of the micelles formed from ($PBYP_{8.5}$-*g*-*ss*-$CPT_{7.5}$)-*b*-$PEEP_{82}$ (scale bar = 200 nm); (B) the particle size distribution curve corresponding to sample (A).

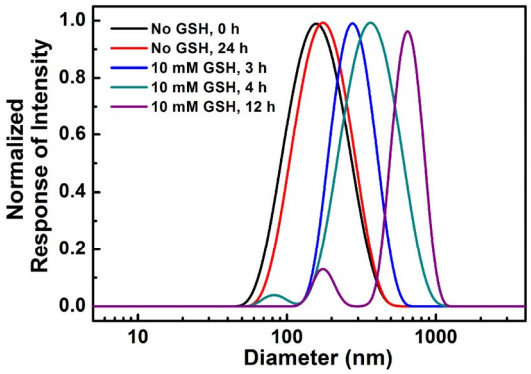

Fig. 10 Time-dependent changes of the micelle size for (PBYP$_{8.5}$-*g*-*ss*-CPT$_{7.5}$)-*b*-PEEP$_{82}$ prodrug micelles at different conditions as determined by DLS.

In vitro drug release

It has been demonstrated that the reduction of disulfide bond generates a thiol intermediate that was expected to be followed by intramolecular cyclization and cleave the neighboring carbonate bridge, thus releasing native CPT molecules from the (PBYP-*g*-*ss*-CPT)-*b*-PEEP micelles. To assess the reduction-responsive release behavior of prodrug micelles, the *in vitro* cumulative release of CTP was investigated under different simulated physiological conditions. The cumulative CPT release results exhibiting a favorable GSH-induced release manner are shown in Fig. 11. For the (PBYP$_{8.5}$-*g*-*ss*-CPT$_{7.5}$)-*b*-PEEP$_{82}$ micelles in the absence of GSH or in the presence of 2 μM GSH, only a minimal CPT release (< 7%) was observed after incubating for 72 h. The result suggests that these prodrug micelles exhibited little drug leakage during blood circulation. In comparison, the CPT releases were significantly accelerated within the same period of time in the presence of 5 mM GSH or 10 mM GSH. Therefore, it is anticipated that these prodrug micelles can realize triggered drug release under the reduction conditions in tumor cell environment.

In vitro cytotoxicity

It is generally known that one of the significant factors for the application of polymeric materials in drug delivery is biocompatibility. PBYP-*b*-PEEP without CPT conjugation exhibited minimal cytotoxicity against L929 cells and HepG2 cells with concentrations up to 200 mg L^{-1}, as shown in Fig. 12, indicating the good biocompatibility of polymers. It has been reported that CPTs interacts with the nuclear protein topoisomerase I and this interferes with the religation of DNA that ultimately leads to cell death.[68] According to the design, the CPT prodrug micelles could be internalized into cells, and CPT parent drug was released triggered by the intracellular reductive environment and diffused into nuclei. Therefore, it is anticipated that (PBYP-*g*-*ss*-CPT)-*b*-PEEP can exhibit antiproliferative activity against tumor cells. The antitumor activity of CPT prodrug micelles against HepG2 cells was investigated using MTT assays. As shown in Fig. 13, (PBYP$_{8.5}$-*g*-*ss*-CPT$_{7.5}$)-*b*-PEEP$_{82}$ exhibited significant cytotoxicity against HepG2 cells and showed an IC$_{50}$ of 0.6 mg L^{-1}, which was higher than that of free CPT (0.36 mg L^{-1}). At the drug concentrations lower than 10 mg L^{-1}, the CPT prodrug micelles showed relatively lower antitumor efficacy as compared to the free CPT. While at the high drug concentrations (>10 mg L^{-1}), the cell viabilities incubated with free CPT displayed a plateau since most of the drug precipitated because of its poor aqueous solubility. It is remarkable that these disulfide-linked CPT prodrug micelles retain relatively high antitumor efficacy, and the reduced cytotoxicity compared with free CPT was likely due to the slower rate of energy-dependent endocytosis and the time-dependent drug release inside the cells following cell internalization.

Cellular uptake

To evaluate the extents of internalization of the prodrug micelles, the cellular internalization of (PBYP-*g*-*ss*-CPT)-*b*-PEEP was then examined against HepG2 cells. The live cell imaging system was introduced to real-time monitor the cellular uptake behaviors. The cell nuclei were stained with NucRed™ Live 647. Since CPT is fluorescent, its emission was directly used to visualize cellular uptake without additional fluorescence probes. Therefore, the amount of CPT prodrug micelles internalized by cells should in principle be proportional to the fluorescence intensity using free CPT as a control. As shown in Fig. 14(A), (PBYP$_{8.5}$-*g*-*ss*-CPT$_{7.5}$)-*b*-PEEP$_{82}$ micelles start to be internalized into HepG2 cells after 6 h incubation and the blue fluorescence intensity of CPT became gradually stronger with the increase of incubation time. After 24 h incubation, a significant portion of prodrug micelles was internalized by HepG2 cells. In comparison, minimal CPT fluorescence was observed in HepG2 cells after being cultured with free CPT for 24 h, as shown in Fig. 14(B). These results indicated that CPT prodrug micelles and free CPT entered into cells in different ways. The prodrug micelles are internalized into cells *via* an endocytosis mechanism. Once the micelles were internalized, it may not be pumped out of the cells during a relatively long period.[69,70] While free CPT entered into tumor cells by a diffusion process depending on the concentration gradient across the cell membrane of tumor cells. Free CPT can enter into cells fast at first, but it is easy for them to escape from the cells later.[71]

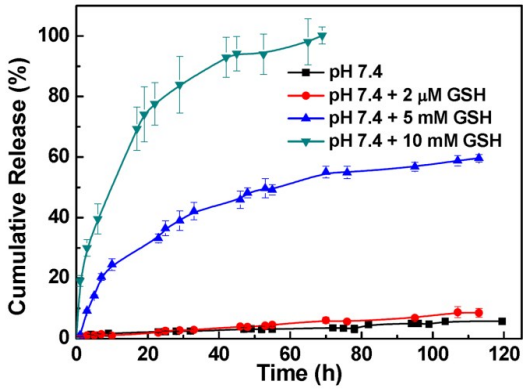

Fig. 11 *In vitro* CPT release from (PBYP$_{8.5}$-*g*-*ss*-CPT$_{7.5}$)-*b*-PEEP$_{82}$ micelles recorded at pH 7.4 and 37 °C under different conditions.

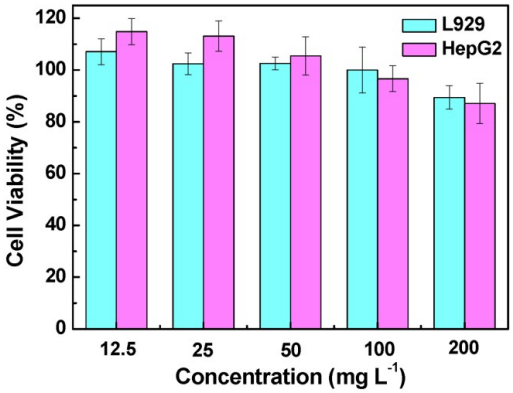

Fig. 12 Cell viability of L929 cells and HepG2 cells treated with $PBYP_{16}$-*b*-$PEEP_{82}$ at different concentrations for 48 h incubation.

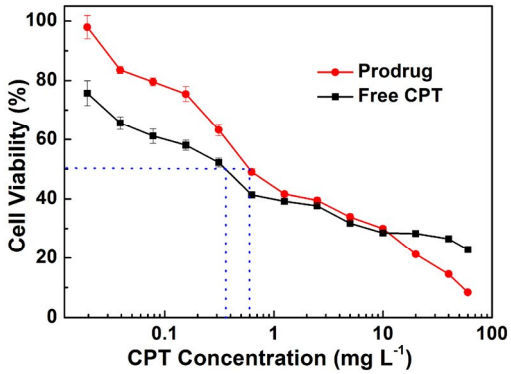

Fig. 13 Cell viability of HepG2 cells treated with ($PBYP_{8.5}$-*g*-*ss*-$CPT_{7.5}$)-*b*-$PEEP_{82}$ and free CPT with different CPT dosages for 48 h incubation.

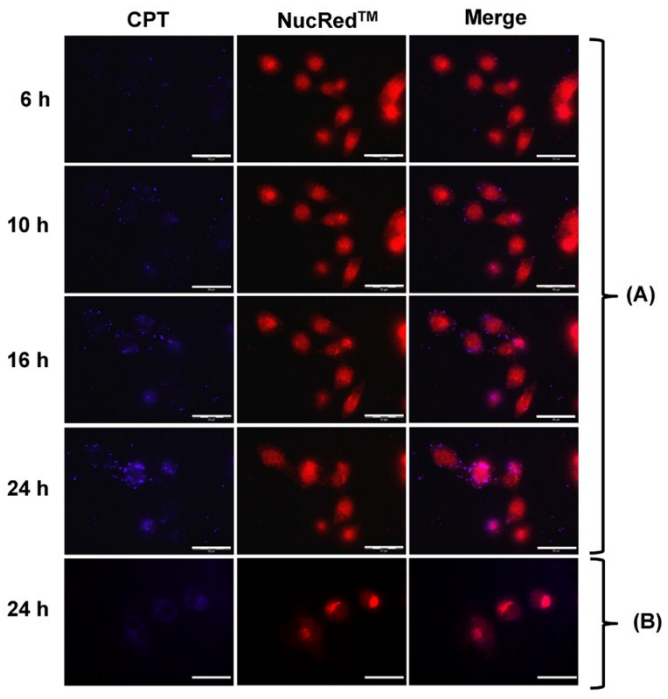

Fig. 14 Fluorescence images of HepG2 cells incubated with (A) ($PBYP_{8.5}$-*g*-*ss*-$CPT_{7.5}$)-*b*-$PEEP_{82}$ micelles following different incubation times and (B) free CPT. The dosage of CPT was 0.5 mg L^{-1}. For each panel, images from left to right show CPT fluorescence in cells (blue), cell nuclei stained by NucRed™ Live 647 and overlays of two images. The scale bars correspond to 50 μm in all the images.

Conclusions

In summary, a novel disulfide-containing polyphosphoester-CPT prodrug (PBYP-*g*-*ss*-CPT)-*b*-PEEP has been successfully synthesized by a combination of ROP and CuAAC "click" reaction. The prodrug could self-assemble into micelles with hydrophobic PBYP segments conjugated CPT as the core and hydrophilic PEEP as the corona with a size of less than 200 nm. MTT assay was used to demonstrate the inhibition efficacy of HepG2 cells proliferation of parent CPT released from these prodrug micelles, which was achieved by the cleavage of disulfide linkage under the tumor-relevant reductive conditions. Moreover, the study by a live cell imaging system further indicated that these prodrug micelles could be internalized into HepG2 cells to deliver the therapeutically active CPT. Overall, this (PBYP-*g*-*ss*-CPT)-*b*-PEEP prodrug with favorable biocompatibility and good reduction sensitivity would be a promising candidate to augment therapeutic efficacy of antitumor drugs and, simultaneously, decrease unfavourable impacts on account of limited biodistribution.

Acknowledgements

The authors gratefully acknowledge financial supports from the National Natural Science Foundation of China (21374066), Suzhou Science and Technology Program for Industrial Application Foundation (SYG201429), a Project Funded by the Priority Academic Program Development (PAPD) of Jiangsu Higher Education Institutions, Soochow-Waterloo University Joint Project for Nanotechnology from Suzhou Industrial Park, and Natural Science Foundation of Jiangsu Higher Education Institutions (13KJB150034). We are also thankful to Professor Jian Liu (FUNSOM, Soochow University) for his kind help in cell-related tests.

Notes and references

1 B. A. Chabner and T. G. Roberts, *Nat. Rev. Cancer,* 2005, **5**, 65-72.
2 D. Peer, J. M. Karp, S. Hong, O. C. Farokhzad, R. Margalit and R. Langer, *Nat. Nanotechnol.*, 2007, **2**, 751-760.
3 K. Riehemann, S. W. Schneider, T. A. Luger, B. Godin, M. Ferrari and H. Fuchs, *Angew. Chem., Int. Ed.*, 2009, **48**, 872-897.
4 K. Kataoka, A. Harada and Y. Nagasaki, *Adv. Drug Delivery Rev.*, 2001, **47**, 113-131.
5 H. Wei, R. X. Zhuo and X. Z. Zhang, *Prog. Polym. Sci.*, 2013, **38**, 503-535.
6 J. S. Lee and J. Feijen, *J. Controlled Release*, 2012, **161**, 473-483.
7 A. V. Kabanov and S. V. Vinogradov, *Angew. Chem., Int. Ed.*, 2009, **48**, 5418-5429.
8 R. Duncan, *Nat. Rev. Cancer*, 2006, **6**, 688-701.
9 F. Kratz, I. A. Müller, C. Ryppa, and A. Warnecke, *ChemMedChem*, 2008, **3**, 20-53.
10 J. Kopeček, *Adv. Drug Delivery Rev.*, 2013, **65**, 49-59.

11 H. Ringsdorf, *J. Polym. Sci. Symposium*, 1975, **51**, 135-153.
12 J. Khandare and T. Minko, *Prog. Polym. Sci.*, 2006, **31**, 359-397.
13 E. Segal and R. Satchi-Fainaro, *Adv. Drug Delivery Rev.*, 2009, **61**, 1159-1176.
14 F. Greco and M. J. Vicent, *Adv. Drug Delivery Rev.*, 2009, **61**, 1203-1213.
15 C. C. Lee, E. R. Gillies, M. E. Fox, S. J. Guillaudeu, J. M. J. Fréchet, E. E. Dy and F. C. Szoka, *Proc. Natl. Acad. Sci. USA*, 2006, **103**, 16649-16654.
16 G. Y. Zhang, M. Z. Zhang, J. L. He and P. H. Ni, *Polym. Chem.*, 2013, **4**, 4515-4525.
17 A. V. Yurkovetskiy and R. J. Fram, *Adv. Drug Delivery Rev.*, 2009, **61**, 1193-1202.
18 Y. Matsumura and H. Maeda, *Cancer Res.*, 1986, **46**, 6387-6392.
19 J. Fang, H. Nakamura and H. Maeda, *Adv. Drug Delivery Rev.*, 2011, **63**, 136-151.
20 T. M. Allen, *Nat. Rev. Cancer*, 2002, **2**, 750-763.
21 J. Nicolas, S. Mura, D. Brambilla, N. Mackiewicz and P. Couvreur, *Chem. Soc. Rev.*, 2013, **42**, 1147-1235.
22 S. Mura, J. Nicolas and P. Couvreur, *Nat. Mater.*, 2013, **12**, 991-1003.
23 R. Cheng, F. H. Meng, C. Deng, H. A. Klok, and Z. Y. Zhong, *Biomaterials*, 2013, **34**, 3647-3657.
24 J. A. MacKay, M. N. Chen, J. R. McDaniel, W. G. Liu, A. J. Simnick and A. Chilkoti, *Nat. Mater.*, 2009, **8**, 993-999.
25 Y. D. Gu, Y. N. Zhong, F. H. Meng, R. Cheng, C. Deng and Z. Y. Zhong, *Biomacromolecules*, 2013, **14**, 2772-2780.
26 Z. G. Xu, K. L. Zhang, C. L. Hou, D. D. Wang, X. Y. Liu, X. J. Guan, X. Y. Zhang and H. X. Zhang, *J. Mater. Chem. B*, 2014, **2**, 3433-3437.
27 X. L. Hu, J. M. Hu, J. Tian, Z. S. Ge, G. Y. Zhang, K. F. Luo and S. Y. Liu, *J. Am. Chem. Soc.*, 2013, **135**, 17617-17629.
28 Y. Y. Zhuang, Y. Su, Y. Peng, D. L. Wang, H. P. Deng, X. D. Xi, X. Y. Zhu and Y. F. Lu, *Biomacromolecules*, 2014, **15**, 1408-1418.
29 Q. G. Wu, F. Du, Y. Luo, W. Lu, J. Huang, J. H. Yu and S. Y. Liu, *Colloids Surf. B*, 2013, **105**, 294-302.
30 X. L. Hu, J. Tian, T. Liu, G. Y. Zhang and S. Y. Liu, *Macromolecules*, 2013, **46**, 6243-6256.
31 A. M. L. Hossion, M. Bio, G. Nkepang, S. G. Awuah and Y. You, *ACS Med. Chem. Lett.*, 2013, **4**, 124-127.
32 H. Liu, Y. L. Li, Z. L. Lyu, Y. B. Wan, X. H. Li, H. B. Chen, H. Chen and X. M. Li, *J. Mater. Chem. B*, 2014, **2**, 8303-8309.
33 M. H. Lee, Z. G. Yang, C. W. Lim, Y. H. Lee, S. DongBang, C. Kang and J. S. Kim, *Chem. Rev.*, 2013, **113**, 5071-5109.
34 G. Y. Wu, Y. Z. Fang, S. Yang, J. R. Lupton and N. D. Turner, *J. Nutr.*, 2004, **134**, 489-492.
35 P. Kuppusamy, H. Q. Li, G. Ilangovan, A. J. Cardounel, J. L. Zweier, K. Yamada, M.C. Krishna and J. B. Mitchell, *Cancer Res.*, 2002, **62**, 307-312.
36 W. H. Lin, X. G. Guan, T. T. Sun, Y. B. Huang, X. B. Jing and Z. G. Xie, *Colloids Surf. B*, 2015, **126**, 217-223.
37 S. Bauhuber, C. Hozsa, M. Breunig and A. Göpferich, *Adv. Mater.*, 2009, **21**, 3286-3306.
38 B. L. Zhang, Z. Luo, J. J. Liu, X. W. Ding, J. H. Li and K. Y. Cai, *J. Controlled Release*, 2014, **192**, 192-201.
39 Y. Zhang, J. L. He, D. L. Cao, M. Z. Zhang and P. H. Ni, *Polym. Chem.*, 2014, **5**, 5124-5138.
40 M. E. Wall, M. C. Wani, C. E. Cook, K. H. Palmer, A. T. McPhail and G. A. Sim, *J. Am. Chem. Soc.*, 1966, **88**, 3888-3890.
41 C. J. Thomas, N. J. Rahier and S. M. Hecht, *Bioorg. Med. Chem.*, 2004, **12**, 1585-1604.
42 J. F. Pizzolato, L. B. Saltz, *Lancet*, 2003, **361**, 2235-2242.
43 Q. Y. Li, Y. G. Zu, R. Z. Shi and L. P. Yao, *Curr. Med. Chem.,* 2006, **13***,* 2021-2039.
44 R. P. Hertzberg, M. J. Caranfa and S. M. Hecht, *Biochemistry*, 1989, **28**, 4629-4638.
45 R. B. Greenwald, A. Pendri, C. D. Conover, C. Lee, Y. H. Choe, C. Gilbert, A. Martinez, J. Xia, D. Wu and M. Hsue, *Bioorg. Med. Chem.*, 1998, **6**, 551-562.
46 T. Schluep, J. J. Cheng, K. T. Khin and M. E. Davis, *Cancer Chemoth. Pharm.*, 2006, **57**, 654-662.
47 H. F. Zhang, J. Q. Wang, W. W. Mao, J. Huang, X. G. Wu, Y. Q. Shen and M. H. Sui, *J. Controlled Release*, 2013, **166**, 147-158.
48 V. R. Caiolfa, M. Zamai, A. Fiorino, E. Frigerio, C. Pellizzoni, R. d'Argy, A. Ghiglieri, M. G. Castelli, M. Farao, E. Pesenti, M. Gigli, F. Angelucci and A. Suarato, *J. Controlled Release*, 2000, **65**, 105-119.
49 E. Kumazawa, and Y. Ochi, *Cancer Sci.*, 2004, **95**, 168-175.
50 R. Bhatt, P. D. Vries, J. Tulinsky, G. Bellamy, B. Baker, J. W. Singer and P. Klein, *J. Med. Chem.*, 2003, **46**, 190-193.
51 S. M. Page, M. Martorella, S. Parelkar, I. Kosif, and T. Emrick, *Mol. Pharmaceutics*, 2013, **10**, 2684-2692.
52 H. Wang, L. Tang, C. L. Tu, Z. Y. Song, Q. Yin, L. C. Yin, Z. H. Zhang, and J. J. Cheng, *Biomacromolecules*, 2013, **14**, 3706-3712.
53 K. W. Leong, H. Q. Mao and R. X. Zhuo, *Chinese J. Polym. Sci.*, 1995, **13**, 289-314.
54 Z. Zhao, J. Wang, H. Q. Mao and K. W. Leong, *Adv. Drug Delivery Rev.*, 2003, **55**, 483-499.
55 Y. C. Wang, Y. Y. Yuan, J. Z. Du, X. Z. Yang and J. Wang, *Macromol. Biosci.*, 2009, **9**, 1154-1164.
56 A. T. Bender and J. A. Beavo, *Pharmacol. Rev.*, 2006, **58**, 488-520.
57 H. W. Duan, D. Y. Wang, D. G. Kurth and H. Möhwald, *Angew. Chem., Int. Ed.*, 2004, **43**, 5639-5642.
58 J. Wen, G. J. A. Kim and K. W. Leong, *J. Controlled Release*, 2003, **92**, 39-48.
59 S. Y. Zhang, A. Li, J. Zou, L. Y. Lin and K. L. Wooley, *ACS Macro Lett.*, 2012, **1**, 328-333.
60 S. Y. Zhang, J. Zou, F. W. Zhang, M. Elsabahy, S. E. Felder, J. H. Zhu, D. J. Pochan and K. L. Wooley, *J. Am. Chem. Soc.*, 2012, **134**, 18467-18474.
61 F. W. Zhang, S. Y. Zhang, S. F. Pollack, R. C. Li, A. M. Gonzalez, J. W. Fan, J. Zou, S. E. Leininger, A. Pavía-Sanders, R. Johnson, L. D. Nelson, J. E. Raymond, M. Elsabahy, D. M. P. Hughes, M. W. Lenox, T. P. Gustafson and K. L. Wooley, *J. Am. Chem. Soc.*, 2015, **137**, 2056-2066.
62 J. Hu, J. L. He, D. L. Cao, M. Z. Zhang and P. H. Ni, *Polym. Chem.*, 2015, **6**, 3205-3216.
63 H. Zhao, Q. J. Chen, L. Z. Hong, L. Zhao, J. F. Wang and C. Wu, *Macromol. Chem. Phys.*, 2011, **212**, 663-672.
64 X. Zhai, W. Huang, J. Y. Liu, Y. Pang, X. Y. Zhu, Y. F. Zhou and D. Y. Yan, *Macromol. Biosci.*, 2011, **11**, 1603-1610.
65 J. L. He, M. Z. Zhang and P. H. Ni, *Soft Matter*, 2012, **8**, 6033-6038.
66 V. Torchilin, *Adv. Drug Delivery Rev.*, 2011, **63**, 131-135.
67 L. F. Zhang and A. Eisenberg, *Science*, 1995, **268**, 1728-1731.
68 T. Andoh, K. Ishii, Y. Suzuki, Y. Ikegami, Y. Kusunki, Y. Takemoto, and K. Okada, *Proc. Nati. Acad. Sci. USA*, 1987, **84**, 5565-5569.
69 L. B. Luo, J. Tam, D. Maysinger and A. Eisenberg, *Bioconjugate Chem.*, 2002, **13**, 1259-1265.
70 R. Savić, L. B. Luo, A. Eisenberg and D. Maysinger, *Science*, 2003, **300**, 615-618.
71 Y. Y. Diao, H. Y. Li, Y. H. Fu, , M. Han, Y. L. Hu, H. L. Jiang, Y. Tsutsumi, Q. C. Wei, D. W. Chen and J. Q. Gao, *Int. J. Nanomed.*, 2011, **6**, 1955-1962.

Journal of Materials Chemistry B

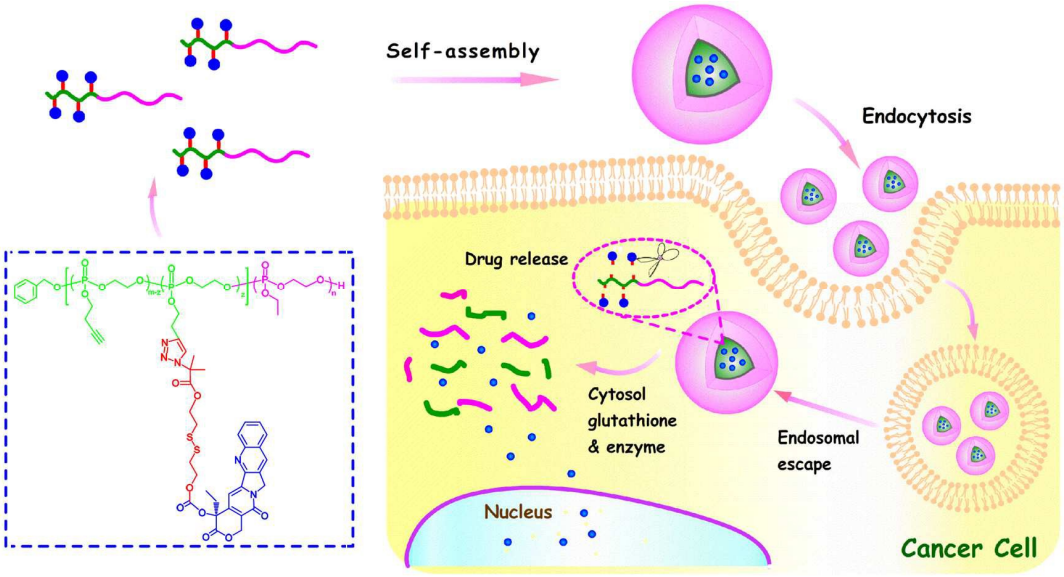

A reduction-cleavable polyphosphoester-camptothecin (CPT) prodrug with tailored drug loading content and triggered drug release has been prepared and applied in tumor chemotherapy.